Int. J. Electrochem. Sci., 16 **(2021)** 151039, doi: 10.20964/2021.01.52

International Journal of
ELECTROCHEMICAL
SCIENCE
www.electrochemsci.org

Synthesis of Organic Acid Doped Polypyrrole and Its Evaluation as a Novel Cathode Material

Pengju Guo[1,*], *Mengtian Ci*[2], *Mayong Zhao*[3]

[1] Shenyang University of Chemical Technology, Shenyang 110000, Liaoning Province, China
[2] Shenyang University of Chemical Technology, Shenyang 110000, Liaoning Province, China
[3] Shenyang University of Chemical Technology, Shenyang 110000, Liaoning Province, China
[*]E-mail: ppjuguo086@163.com

Received: 20 September 2020 / *Accepted:* 7 November 2020 / *Published:* 30 November 2020

Using pyrrole and benzene carboxylic acid as raw materials, composite materials (BeAcLi/PPy) were successfully prepared by redox method. The structures, morphologies and battery performances of PPy and the composite materials (BeAcLi/PPy) were obtained with FTIR, SEM, CV and EIS. Battery performances of PPy and composite materials (BeAcLi/PPy) were obtained with a constant charge/discharge current. Test results revealed that PPy and the composite materials (BeAcLi/PPy) had reversible redox processes from 2.0-4.0 V. The discharge specific capacities of BeAcLi/PPy (3:1) and BeAcLi/PPy (5:1) were 74.5 and 57.8 $mAh \cdot g^{-1}$, respectively, as measured at 20 $mA \cdot g^{-1}$ between 2.0 and 4.0 V; these results were evidently better than that of PPy (29.7 $mAh \cdot g^{-1}$) under identical experimental conditions. Additionally, the rate performances and cycling performances of the composite materials significantly improved. The excellent electrochemical performances of composite materials were mainly due to the introduction of BeAcLi as a dopant, thereby improving the polarization of PPy. In addition, the prepared composite materials had a uniform and open loosely stacked structure, which was conducive for increasing contact area between electrode material and electrolyte. As a result, the availability of active material improved, and the electrochemical properties improved.

Keywords: Lithium-ion battery; Dopant; Pyrrole; Electrode material; Composite materials

1. INTRODUCTION

With the rapid development of emerging fields, such as power vehicles, smart grids, and 3C products, lithium-ion batteries (LIBs), which have exhibit cycling stability and excellent specific capacity, play a vital role. To satisfy the increasing requirements for electricity in current society, lithium-ion batteries not only have abundant opportunities but also tremendous challenges. Traditional electrode materials are generally metal oxides, such as $LiCoO_2$, $LiNiO_2$, and $LiFePO_4$. [1] Metal oxide

electrode materials have limited theoretical specific capacities; furthermore, metals pollute the environment and mineral resources are limited. [2-4] Alternatively, organic materials with redox properties are ideal substitutes for charge storage materials because they are renewable resources compared to traditional electrode materials; additionally, they are also environmentally friendly and inexpensive. Therefore, many researchers have increasingly studied organic materials with redox activity as electrode materials for use in lithium-ion batteries or supercapacitors. Organic materials mainly include organic radical compounds, [5-6] organic sulfur compounds, [7] conductive polymers [8-9] and organic carbonyl compounds. [10-14]

Among all these organic materials, conductive polymers and composite materials have become promising electrode materials due to their own low bandgap, good inherent conductivity, fast charging/discharging capabilities and low cost. [15-16] Extensive studies have shown that polypyrrole (PPy), polythiophene (PTh), etc. can achieve excellent energy storage performance and have a unique π-electron conjugated skeleton structure when formed as conductive polymers. [13] As a well-known conductive polymer, PPy has been widely used in battery research. [17] Polypyrrole has high conductivity and good stability under environmental conditions; moreover, polypyrrole is easy to synthesize. Therefore, PPy has attracted widespread attention from scientific researchers. The theoretical capacity of PPy is 412 $mAh.g^{-1}$ under fully doped conditions, which is equivalent to $LiCoO_2$, an organic silicon electrode material. However, realistic discharge capacity of PPy is lower than theoretical discharge capacity, which results in limiting its application and cannot be successfully used in commercial batteries. [18-20] The main cause for the decline in electrochemical performance of PPy is its tendency to seriously aggregate, which lowers the utilization rate of active materials and leads to low conductivity and the lower actual electrochemical activity of PPy. [21] In addition, the electrochemical performance of PPy is connected to its degree of doping, and agglomerated PPy prevents the electrolyte from diffusing into the active material, resulting in a lower doping level and specific discharge capacity. [22]

To settle these difficult problems, researchers have suggested that PPy should be doped with electroactive groups to effectively improve the aggregation morphology of the polymer, thereby enhancing its electrochemical performance. [23-24] In addition, some anions act as dopants. Ren's research team used nanosilica modified with a silane coupling agent (APS) as a dopant and successfully prepared a composite electrode material (PPy/APS-SiO_2). [25] The results showed that the electrochemical properties improved (see Table 1). The improvement in electrochemical performance was mainly attributed to introduction of dopants effectively improving agglomeration morphology of PPy, thereby promoting the more efficient use of electrode materials. [25] Additionally, organic acid-doped polypyrrole has attracted considerable research attention. Organic acid-doped polypyrrole (such as molybdate [26] and ferrocene carboxylic acid [9]) can induce more convenient charge transfer, thereby improving utilization of active material and electrochemical performance (see Table 1). Therefore, appropriately selecting organic dopants for conductive polymers that will be used as electrode materials is vital to acquire excellent electrochemical performance. In addition, some studies have shown that the establishment of an open topographic structure can effectively help the contact area between the active site and electrolyte, thereby improving electrochemical performance. [27-29]

Therefore, it is very important to select appropriate organic dopants to obtain efficient composite electrode materials to improve electrochemical performance.

In this article, we first prepared an organic acid dopant, lithiated benzoic acid (BeAcLi), and then copolymerized the dopant and pyrrole by a redox method to acquire composite materials (BeAcLi/PPy). Then, the prepared composite electrode materials were used as cathode materials, and the battery performances of these composite materials were further discussed in detail. Therefore, we prepared composite materials using different molar ratios and studied battery performance of these composite electrode materials. Results showed that compared with pure PPy, battery performance of BeAcLi/PPy was significantly improved. The discharge specific capacity of BeAcLi/PPy (5:1) was 57.8 $mAh \cdot g^{-1}$, which was much higher than PPy (29.7 $mAh \cdot g^{-1}$). In particular, when the composite electrode material BeAcLi/PPy (3:1) was used as the cathode, the battery performance was superior (see Table 1). From Table 1, we can see that BeAcLi/PPy (3:1) exhibited a higher specific discharge capacity (74.5 $mAh \cdot g^{-1}$) compared with other composite electrode materials. Precise data of specific discharge capacity about PPy/APS-SiO_2, PPy/MO and PPy/ferrocene are 40 $mAh \cdot g^{-1}$, 62 $mAh \cdot g^{-1}$ and 65 $mAh \cdot g^{-1}$, respectively. [25, 26, 9] Therefore, these results also showed that BeAcLi as a dopant was more favourable in improving the electrochemical performance of PPy. This result was mainly due to the improved morphology after the introduction of BeAcLi and the successful construction of a uniform and open loosely stacked structure, which could effectively help the contact between the active site and electrolyte; thus, the electrochemical performance was improved.

Table 1. Precise data of composite electrode materials prepared by various dopants

Dopant	APS-SiO_2	Molybdate	Ferrocene carboxylic acid	BeAcLi
Composite material	PPy/APS-SiO_2 [25]	PPy/MO [26]	PPy/ferrocene [9]	BeAcLi/PPy (3:1)
Specific discharge capacity	40$mAh \cdot g^{-1}$	62 $mAh \cdot g^{-1}$	65 $mAh \cdot g^{-1}$	74.5 $mAh \cdot g^{-1}$

2. EXPERIMENT

2.1. Material synthesis

Benzoic acid (AR) and LiOH (AR) were purchased from Shanghai Aladdin Biochemical Technology Co., Ltd. Pyrrole (AR), acetonitrile (AR), ammonium persulfate (AR) and HCl (AR) were purchased from Sinopharm Chemical Reagent Co., Ltd.

2.2. Preparation of composite materials (BeAcLi/PPy)

First, we lithiated benzoic acid with LiOH at a molar ratio of 1:1. Then, we adjusted it to a neutral pH using hydrochloric acid. Thus, lithiated benzoic acid (BeAcLi) was obtained. Second, we dissolved pyrrole (0.2 g) and different amounts of BeAcLi using a mixed solvent of deionized water

(15 ml) and acetonitrile (3 ml). Using ammonium persulfate as oxidant, reaction was carried out at normal temperature for 7 hours. The product was washed with water and then dried in vacuum box for 48 hours. Finally, the black composite materials, BeAcLi/PPy (3:1) and BeAcLi/PPy (5:1), were obtained.

2.3. Material characterization

SEM was tested with JEOL JSM7200F scanning electron microscope. FTIR was tested with Nicolet IS10 spectrometer (Thermo Fisher Scientific, Inc.), and KBr was used for tablet compression.

2.4. Electrochemical measurements

A CR2025 button battery was prepared in a super-purified glove box filled with argon while ensuring that the contents of water and O_2 were both below 0.1 ppm. The cathode electrode was made of composite material (BeAcLi/PPy) as the active material, acetylene black as conductive agent, PVDF as binder and NMP as solvent. The electrode material, acetylene black and PVDF were mixed and stirred at a mass ratio of 60:30:10, and then this uniformly ground electrode material was smeared on pretreated aluminium foil. Next, the coated aluminium foil was dried under vacuum at 70°C for 24 hours. Finally, assembled CR2025 button battery was installed in LAND CT2001A instrument. Voltage range was 2.0–4.0 V, and the test was performed at constant current rate. CV and EIS were conducted with CHI 760E electrochemical workstation (Shanghai Chenhua Instrument Co., Ltd.)

3. RESULT AND DISCUSSION

3.1. Material characterization

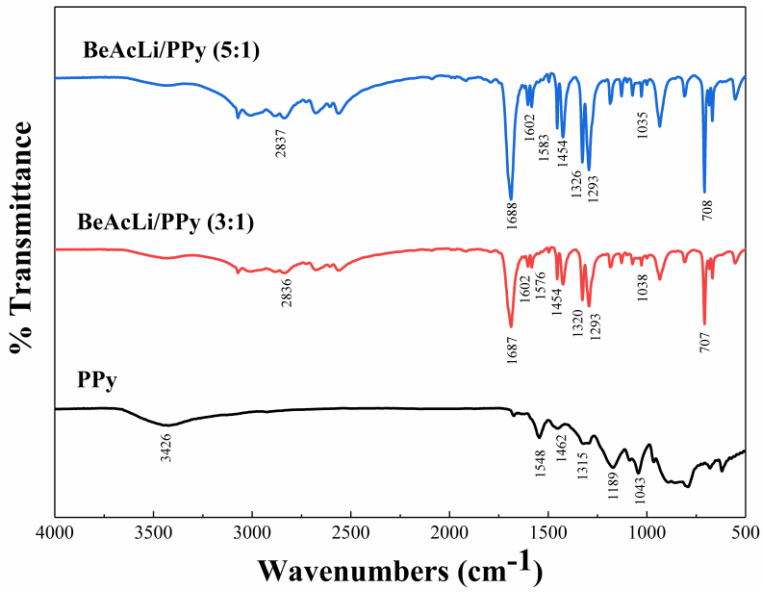

Figure 1. FTIR spectrum of PPy, BeAcLi/PPy (3:1) and BeAcLi/PPy (5:1) samples.

Figure 1 shows FTIR spectra of PPy, BeAcLi/PPy (3:1) and BeAcLi/PPy (5:1). The representative characteristic peak of PPy can be found in the sample. The symmetric and asymmetric stretching vibration peaks of pyrrole ring are at 548 and 1462 cm^{-1}, and peaks at 1315 and 1043 cm^{-1} are the C-H in-plane vibrations, which are consistent with the conclusion of the representative peaks of PPy in the literature. [30] The CN stretching vibrations are at 925 and 788 cm^{-1}. Additionally, the composite materials BeAcLi/PPy (3:1) and BeAcLi/PPy (5:1) show similar characteristic bands in the test results, but these bands are blueshifted compared with those of PPy. This result indicates that the doping of BeAcLi is beneficial for improving the morphology of PPy and results in a smoother charge transfer. Moreover, BeAcLi/PPy (3:1) and BeAcLi/PPy (5:1) exhibit characteristic peaks of carbonyl groups, benzene rings and pyrrole units. The 1687 cm^{-1} peak corresponds to stretching vibration peak of C=O double bond. Stretching vibration peaks of aromatic ring skeleton are at 1602 and 1454 cm^{-1}, and peak at 1293 cm^{-1} is the C-H stretching vibration peak, which is in accordance with result of the benzene ring mentioned in the literature. [31] Therefore, these results also prove that BeAcLi has been successfully doped into the polypyrrole fragments.

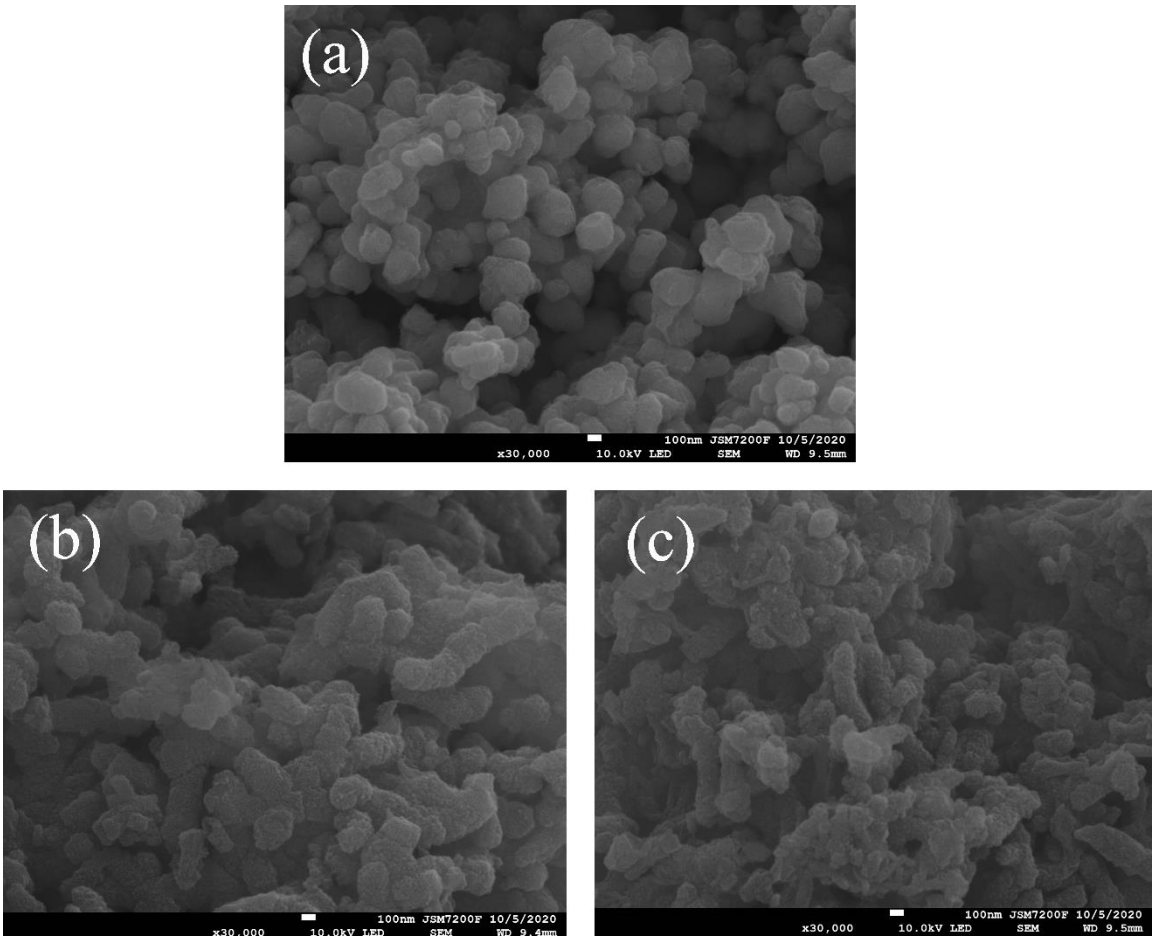

Figure 2. SEM images of (a) PPy, (b) BeAcLi/PPy (3:1), and (c) BeAcLi/PPy (5:1).

Figure 2 shows SEM showing morphologies of PPy, BeAcLi/PPy (3:1) and BeAcLi/PPy (5:1). As shown in Figure 2a, PPy has a close, crowded structure of particles, and its particle size range is 200-300 nm. This result is consistent with the particle size of PPy, which is 256 nm in the literature.

[32] When BeAcLi is incorporated into the polypyrrole framework as a dopant, the prepared composite material (BeAcLi/PPy) exhibits a loosely distributed morphology. In particular, the morphology of the composite material BeAcLi/PPy (3:1) is improved significantly, exhibiting a uniform and open loosely stacked morphology with a strip structure (as shown in Figure 2b). However, with the further increase in the amount of BeAcLi, the loosely stacked morphology of the BeAcLi/PPy (5:1) composite weakens due to the excessive doping of BeAcLi (as shown in Figure 2c). Thus, the uniform and open loosely stacked morphology of BeAcLi/PPy greatly improves performance of material in batteries.

3.2. Electrochemical performance

To assess electrochemical performance, we obtained CV curves of the materials. Figure 3 reveals CV curves of PPy, BeAcLi/PPy (3:1) and BeAcLi/PPy (5:1). The scanning rate was 1 mV/s, and potential range was 2.0-4.0 V. The CV curve of PPy shows redox peaks (3.416/2.993 V) in the scan, which are associated with the redox reaction of the pyrrole unit. The symmetrical and wide CV chart also reflects the capacitor behaviour of PPy. [33] Compared with the original PPy, the composite material (BeAcLi/PPy) exhibits a larger redox peak area, which indicates that the composite material has better electrochemical performance.

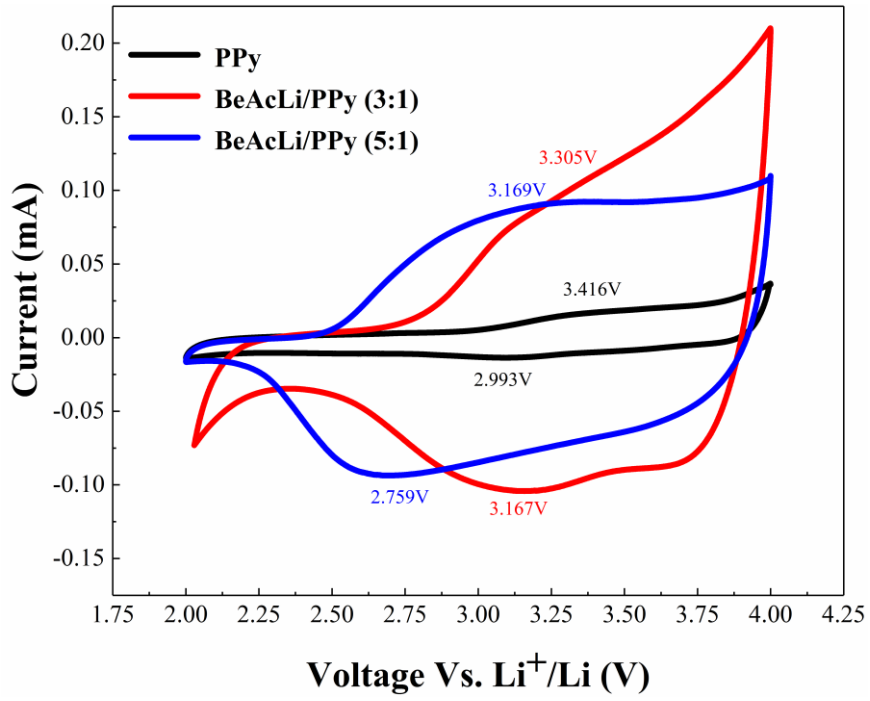

Figure 3. CV curves of PPy, BeAcLi/PPy (3:1) and BeAcLi/PPy (5:1) at a scan rate of 1 mV/s.

In addition, Figure 3 shows that redox peak of BeAcLi/PPy (3:1) is 3.305/3.167 V. The oxidation/reduction peak of BeAcLi/PPy (5:1) is 3.169/2.759 V. Additionally, the difference between the anode and cathode peaks of PPy, BeAcLi/PPy (3:1) and BeAcLi/PPy (5:1) are 0.423, 0.138 and 0.41 V, respectively. Yang's research team prepared a PPy/MO composite electrode material. [26]

During the electrochemical performance test, the redox peak difference and discharge specific capacity of PPy/MO were 0.4 V and 62 $mAh \cdot g^{-1}$, respectively. [26] Compared with PPy/MO, the peak difference of BeAcLi/PPy (3:1) is smaller, and BeAcLi/PPy (3:1) exhibits a higher specific discharge capacity (74.5 $mAh \cdot g^{-1}$). These results show that the composite material BeAcLi/PPy (3:1) has the smallest polarization, which is favourable for reversible electrochemical reactions and helps to improve its electrochemical performance. In summary, BeAcLi/PPy (3:1) shows the highest peak area and the smallest polarization. This result is mainly due to the introduction of dopants to improve the particle packing morphology of polypyrrole. The uniform and open loosely stacked structure of the composite material BeAcLi/PPy (3:1) can help insertion/extraction of Li^+ and increase contact area of Li^+ andPF_6^- with more active sites on electrode material during charging/discharging. Therefore, the composite material BeAcLi/PPy (3:1) shows better electrochemical performance.

3.3. Charge-discharge performance

To explore reversible electrochemical performance of PPy, BeAcLi/PPy (3:1) and BeAcLi/PPy (5:1), we conducted a cycling performance test using a constant current of 20 $mA \cdot g^{-1}$. Figure 4a is initial charge/discharge curve. From Figure 4a, we can conclude that pure PPy has a smaller specific discharge capacity (29.4 $mAh \cdot g^{-1}$), indicating that the PPy electrode undergoes redox reactions during charge-discharge, which is supported by the literature. [34] In comparison, BeAcLi/PPy (3:1) and BeAcLi/PPy (5:1) show high specific discharge capacities of 75.6 and 50.3 $mAh \cdot g^{-1}$, respectively, which are far higher than pure PPy. At the same time, literature reports mention that the specific discharge capacities of composite electrode materials PPy/MO, PPy/ferrocene, and BeAcLi/PPy (3:1) are 40$mAh \cdot g^{-1}$, 62 $mAh \cdot g^{-1}$, 65 $mAh \cdot g^{-1}$, respectively. [9, 25, 26] However, BeAcLi/PPy (3:1) exhibits a higher specific discharge capacity (74.5 $mAh \cdot g^{-1}$), which is also consistent with CV. In particular, BeAcLi/PPy (3:1) clearly shows a higher specific discharge capacity than other materials. This result is mainly due to the suitable doping process that effectively improves the morphology of PPy and effectively improves the contact of redox active material and electrolyte during charging/discharging.

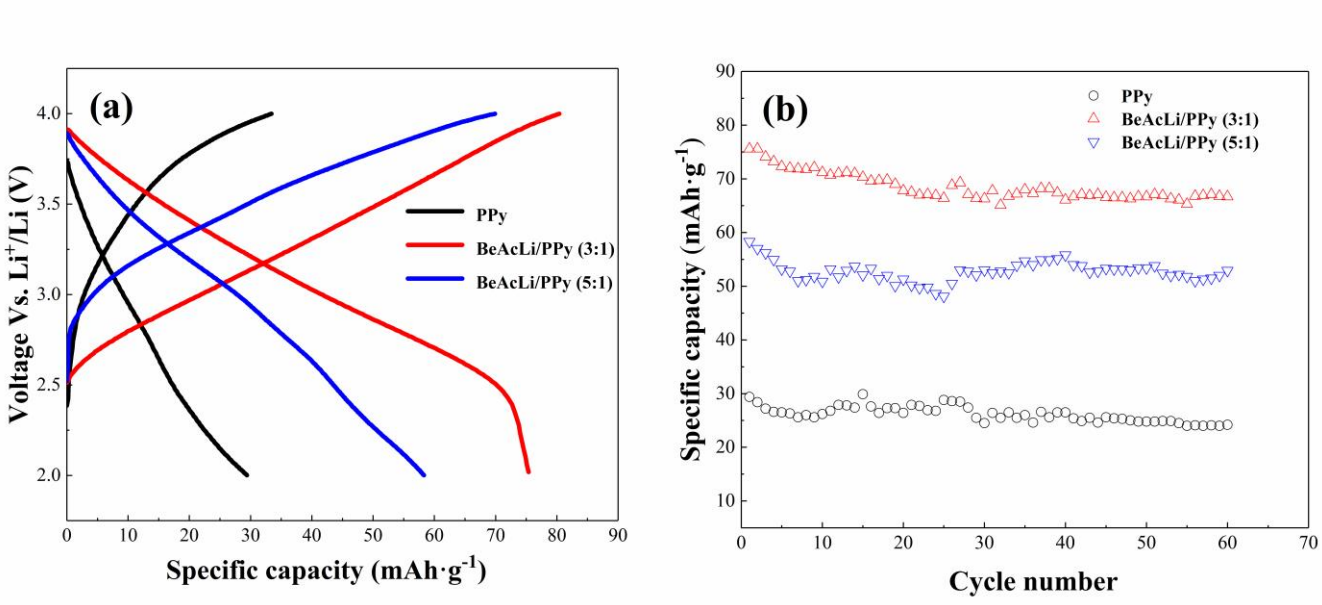

Figure 4. (a): initial cycle charge/discharge profiles and (b): cycling stability at a constant current of 20 mA/g from 2-4 V.

The cycling stability of PPy, BeAcLi/PPy (3:1) and BeAcLi/PPy (5:1) is revealed in Figure 4b. From Figure 4b, we can see that specific discharge capacity of PPy changes from 29.4 to 24.2 $mAh \cdot g^{-1}$ after 60 cycles, and capacity loss is approximately 17.7%. In regard to the composite material BeAcLi/PPy (5:1), the specific discharge capacity decreases significantly after 60 cycles. In contrast, BeAcLi/PPy (3:1) has better cycling stability, and the specific discharge capacity becomes 66.7 $mAh \cdot g^{-1}$ after 60 cycles, indicating that BeAcLi/PPy (3:1) has a stable morphology and chemical structure during charging/discharging. In summary, it can be seen that proper doping can make the composite material BeAcLi/PPy (3:1) build a stable morphological structure, which is beneficial for improving cycling stability and the specific discharge capacity. Moreover, the uniform and open loosely stacked morphology facilitates contact between the electrode material and electrolyte, thereby increasing discharge specific capacity.

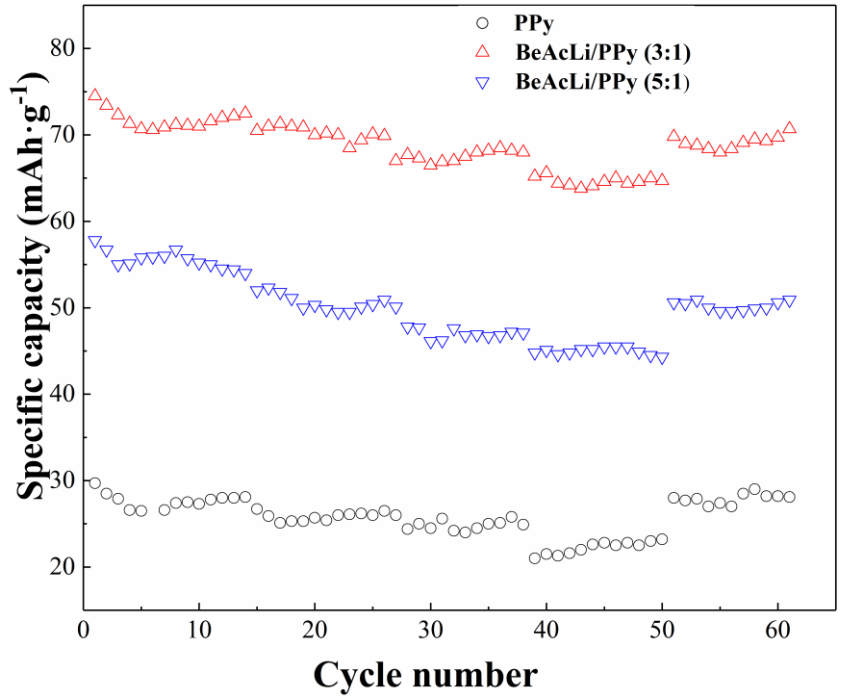

Figure 5. Cycling stability of PPy, BeAcLi/PPy (3:1) and BeAcLi/PPy (5:1) at different current rates of 20, 50, 100, 200, and 20 $mA \cdot g^{-1}$ from 2-4.0 V.

In addition, we also tested the rate performance of PPy and the composite materials (BeAcLi/PPy), and potential range was 2.0-4.0 V. Figure 5 shows that the specific discharge capacities of PPy and the composite materials (BeAcLi/PPy) gradually decrease with an increasing current rate, which is attributed to the increased polarization effect. Discharge capacity of PPy is 29.7, 26.7, 24.5 and 22.5 $mAh \cdot g^{-1}$ at current rates of 20, 50, 100 and 200 $mA \cdot g^{-1}$, respectively. Current rate increases from 20 to 200 $mA \cdot g^{-1}$, and specific discharge capacity loss is 24.2%. In regard to the composite materials (BeAcLi/PPy), they show better specific discharge capacities under identical current rates. In addition, BeAcLi/PPy (3:1) has best rate performance and higher discharge capacity retention rate. At a current rate of 200 $mA \cdot g^{-1}$, BeAcLi/PPy (3:1) can also supply specific discharge capacity of 66.2 $mAh \cdot g^{-1}$, with specific capacity retention rate of 88.9%. In addition, BeAcLi/PPy (3:1) also has better stability during specific discharge capacity recovery, and when current density finally returns to 20 $mA \cdot g^{-1}$, specific discharge capacity recovers to 70.2 $mAh \cdot g^{-1}$, which is approximately 94.3% of the original specific discharge capacity. This result is mainly because the introduction of organic acid dopants enhances the morphological structure of PPy, which is beneficial for improving the cycling stability of the material. At the same time, the uniformly dispersed loose microstructure of BeAcLi/PPy (3:1) makes it easier for the electrolyte to penetrate into the active material, thereby increasing contact area between electrolyte and active material. This contact results in a further reduction in polarization and improved electrochemical performance. In addition, as shown in Figure 6, the composite material (BeAcLi/PPy) electrode still shows an obvious and stable voltage distribution at 200 $mA \cdot g^{-1}$, which means that the composite material (BeAcLi/PPy) has stable structure and low polarization during charge-discharge process.

Figure 7 shows EIS results of PPy, BeAcLi/PPy (3:1) and BeAcLi/PPy (5:1). The electrochemical impedance chart consists of a semicircular high-frequency region and a linear low-frequency region.

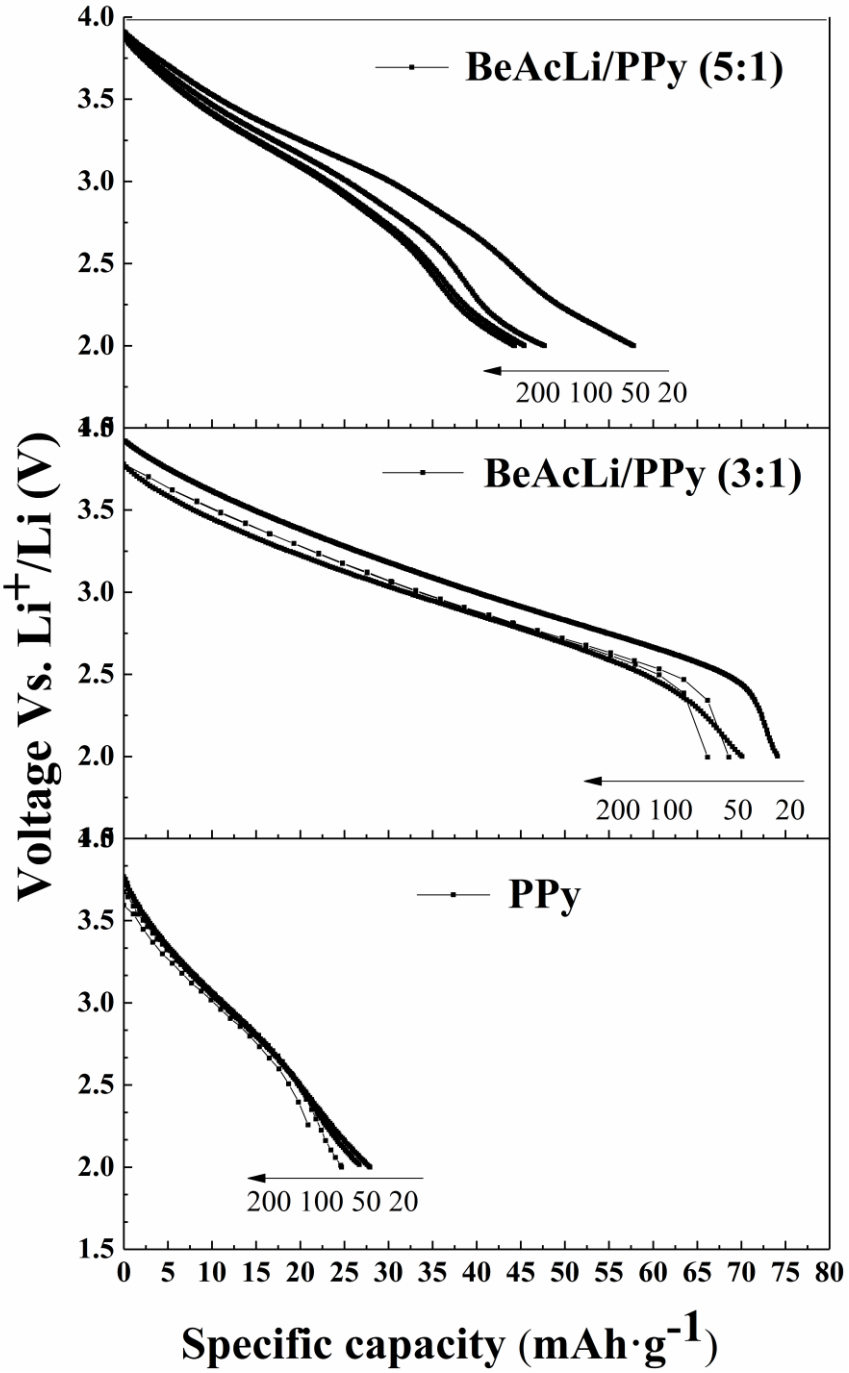

Figure 6. Initial discharge curves of PPy, BeAcLi/PPy (3:1) and BeAcLi/PPy (5:1) at different current rates of 20, 50, 100, 200, and 20 $mA \cdot g^{-1}$ from 2-4.0 V.

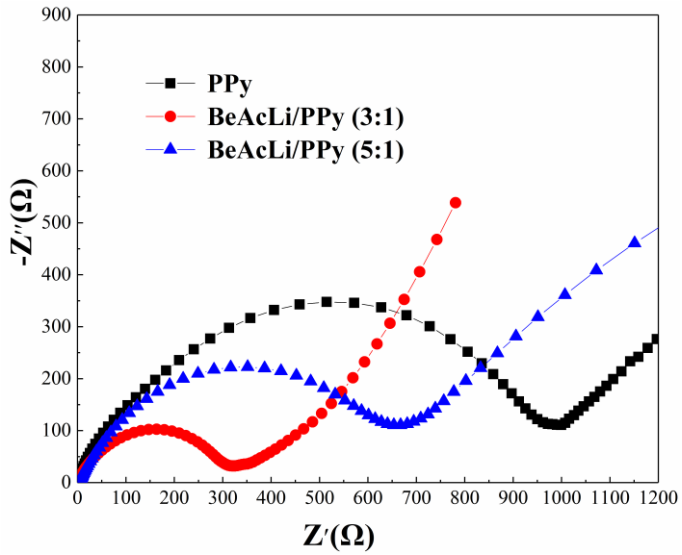

Figure 7. EIS curves of PPy, BeAcLi/PPy (3:1) and BeAcLi/PPy (5:1) electrodes.

The semicircular high-frequency region is charge transfer resistance, while the sloping line in low-frequency region is attributed to diffusion of Li^+ in active material. [35] Sultana's research team proposed that a small charge transfer resistance was conducive to charge transfer, thereby improving telectrochemical properties of material. [36] This conclusion is consistent with the test results in this article. The results also verify the excellent electrochemical performance of BeAcLi/PPy (3:1). The test results show that charge transfer resistances of PPy, BeAcLi/PPy (3:1) and BeAcLi/PPy (5:1) are 972.2, 311.9 and 653.7 Ω, respectively. Among them, BeAcLi/PPy (3:1) has the lowest resistance. The low impedance of BeAcLi/PPy (3:1) facilitates improved charge transfer when used as an electrode during electrochemical process, which is consistent with improved electrochemical performance results of BeAcLi/PPy (3:1). This improvement indicates that the stable chemical morphology and the uniform and open loosely stacked morphology formed by the composite material BeAcLi/PPy (3:1) help improve electron transport and ion diffusion, leading to a low charge transfer resistance. This low resistance is also reason that composite material BeAcLi/PPy (3:1) shows good battery performance.

4. CONCLUSION

Composite materials (BeAcLi/PPy) were first prepared by using BeAcLi as a dopant. The prepared composite material BeAcLi/PPy (3:1) has a uniform and open loosely stacked morphology, which is conducive to the insertion/extraction of Li^+. During the battery performance test, the composite material (BeAcLi/PPy) shows better battery performance. In particular, BeAcLi/PPy (3:1) exhibits a discharge specific capacity of 74.5 $mAh \cdot g^{-1}$ at 20 $mA \cdot g^{-1}$, which is significantly higher than that of other two tested materials. At the same time, BeAcLi/PPy (3:1) has a more stable rate performance and good cycling capacity, with the capacity recovery rate being 94.3%. The excellent electrochemical performance of the composite material BeAcLi/PPy (3:1) is mainly attributed to the introduction of BeAcLi to build a stable morphological structure, which helps to improve specific

discharge capacity and cycling stability. At the same time, the uniform and open loosely stacked morphology is more conducive to providing increased contact area between the active material and electrolyte, thereby increasing specific discharge capacity.

References

1. M. Armand and J. M. Tarascon, *Nature*, 451 (2008) 652.
2. P. L. Taberna, S. Mitra, P. Poizot, P. Simon and J. M. Tarascon, *Nat. Mater.*, 5 (2006) 567.
3. N. Du, H. Zhang, B. D. Chen, J. B. Wu, X. Y. Ma, Z. H. Liu, Y. Q. Zhang, D. R. Yang, X. H. Huang and J. P. Tu, *Adv. Mater.*, 19 (2007) 4505.
4. H. Li, Z. X. Wang, L. Q. Chen and X. J. Huang, *Adv. Mater.*, 21 (2009) 4593.
5. T. Janoschka, M. D. Hager and U. S. Schubert, *Adv. Mater.*, 24 (2012) 6397.
6. W. Guo, Y. X. Yin, S. Xin, Y. G. Guo and L.J. Wan, *Energy & Environ. Sci.*, 5 (2012) 5221.
7. Y. J. Li, H. Zhan, L. B. Kong, C. M. Zhan and Y. H. Zhou, *Electrochem. Commun.*, 9 (2007) 1217.
8. N. Oyama, T. Tatsuma, T. Sato and T. Sotomura, *Nature*, 373 (1995) 598.
9. K. S. Park, S. B. Schougaard and J. B. Goodenough, *Adv. Mater.*, 19 (2007) 848.
10. T. Nokami, T. Matsuo, Y. Inatomi, N. Hojo, T. Tsukagoshi, H. Yoshizawa, A. Shimizu, H. Kuramoto, K. Komae, H. Tsuyama and J. I. Yoshida, *J. Am. Chem. Soc.*, 134 (2012) 19694.
11. Z. Q. Zhu, M. L. Hong, D. S. Guo, J. F. Shi, Z. L. Tao and J. Chen, *J. Am. Chem. Soc.*, 136 (2014) 16461.
12. W. Luo, M. Allen, V. Raju and X. L. Ji, *Adv. Energy Mater.*, 4 (2014) 1400554.
13. X. Han, C. Chang, L. Yuan, T. Sun and J. Sun, *Adv. Mater.*, 19 (2007) 1616.
14. T. L. Gall, K. H. Reiman, M. C. Grossel and J. R. Owen, *J. Power Sources*, 119 (2003) 316.
15. C. Peng, S. G. Zhang, D. Jewell and G. Z. Chen, *Prog. Nat. Sci.*, 18 (2008) 777.
16. G. A. Snook, P. Kao and A. S. Best, *J. Power Sources*, 196 (2011) 1.
17. J. Q. Wang, J. Liu, M. M. Hu, J. Zeng, Y. B. Mu, Y. Guo, J. Yu, X. Ma, Y. J. Qiu and Y. Huang, *J. Mater. Chem. A.*, 6 (2018) 11113.
18. P. Novák and W. Vielstich, *J. Electrochem. Soc.*, 137 (1990) 1681.
19. M. D. Levi, Y. Gofer and D. Aurbach, *Polym. Advan. Technol.*, 13 (2002) 697.
20. J. Z. Wang, S. L. Chou, H. Liu, G. X. Wang, C. Zhong, S. Y. Chew and H.K. Liu, *Mater. Lett.*, 63 (2009) 2352.
21. K. Naoi, M. M. Lien and W. H. Smyrl, *J. Electroanal. Chem. Interfa. Electrochem.*, 272 (1989) 273.
22. T. F. Otero, H. Grande and J. Rodríguez, *J. Electroanal. Chem.*, 394 (1995) 211.
23. B. L. Ellis, P. Knauth and T. Djenizian, *Adv. Mater.*, 26 (2014) 3368.
24. A. A. Khan and L. Paquiza, *Synth. Met.*, 161 (2011) 899.
25. L. Ren, G. X. Cheng, L. X. Wang, C. Zhu, *J. Funct. Mater.*, 36 (2005) 613.
26. Y. Xiong, M Zhou, J. F. Qian, H. X. Yang, *Chinese Sci. Bull.*, 58 (2013) 3336.
27. T. Nokami, T. Matsuo, Y. Inatomi, N. Hojo, T. Tsukagoshi, H. Yoshizawa, A. Shimizu, H. Kuramoto, K. Komae, H. Tsuyama and J. I. Yoshida, *J. Am. Chem. Soc.*, 134 (2012) 19694.
28. W. Walker, S. Grugeon, H. Vezin, S. Laruelle, M. Armand, F. Wudl and J. M. Tarascon, *J. Mater. Chem.*, 21 (2011) 1615.
29. P. Nesvadba, L. B. Folger, P. Maire and P. Novák, *Synth. Met.*, 161 (2011) 259.
30. X. Liang, Y. Liu, Z. Y. Wen, L. Z. Huang, X. Y. Wang, H. P. Ai, H. Zhang, *J. Power Sources*, 196 (2011) 6951.
31. J. Ni, K. J. Wei, Y. Z. Liu, X. C. Huang, D. Li, *Cryst. Growth Des.*, 10 (2010) 3964.
32. G. Wang, L. Yang, Q. Qu, B. Wang, Y. Wu, R. Holze, J. Solid State Electr., 14 (2010) 865.
33. D. P. Dubal, S. H. Lee, J. G. Kim, W. B. Kim and C. D. Lokhande, *J. Mater. Chem.*, 22 (2012) 3044.

34. S. Biswas and L. T. Drzal, *Chem. Mater.,* 22 (2010) 5667.
35. J. X. Li, M. Z. Zou, Y. Zhao, Y. B. Lin, H. Lai, L. H. Guan and Z.G. Huang, *Electrochim. Acta,* 111 (2013) 165.
36. I. Sultana, M. M. Rahman, J. Z. Wang, C. Y. Wang, G. G. Wallace, H. K. Liu, *Solid State Ion.,* 215 (2012) 29.